

averaging of the cross-correlated relaxation rate which may reveal slow motion up to 1 ms.

## REFERENCES AND NOTES

1. K. Wüthrich, *NMR of Proteins and Nucleic Acids* (Wiley, New York, 1986).
2. I. Solomon, *Phys. Rev.* **99**, 559 (1955); \_\_\_\_\_ and N. Bloembergen, *J. Chem. Phys.* **25**, 261 (1956).
3. M. Karplus, *J. Chem. Phys.* **30**, 11 (1959); *J. Am. Chem. Soc.* **85**, 2870 (1963).
4. C. Griesinger, O. W. Sørensen, R. R. Ernst, *J. Magn. Reson.* **73**, 574 (1987); *J. Am. Chem. Soc.* **109**, 7227 (1987); H. Oschkinat *et al.*, *Nature* **332**, 374 (1988); M. Ikura, L. E. Kay, A. Bax, *Biochemistry* **29**, 4659 (1990); L. E. Kay, G. M. Clore, A. Bax, A. M. Gronenborn, *Science* **249**, 411 (1990); M. Ikura, A. Bax, G. M. Clore, A. M. Gronenborn, *J. Am. Chem. Soc.* **112**, 9020 (1990); G. M. Clore, L. E. Kay, A. Bax, A. M. Gronenborn, *Biochemistry* **30**, 12 (1991); E. R. P. Zuiderweg, A. M. Petros, S. W. Fesik, E. T. Olejniczak, *J. Am. Chem. Soc.* **113**, 370 (1991); G. M. Clore and A. M. Gronenborn, *Science* **252**, 1390 (1991).
5. B. H. Oh, W. M. Westler, P. Darba, J. L. Markley, *Science* **240**, 908 (1988); E. P. Nikonowicz *et al.*, *Nucleic Acids Res.* **20**, 4507 (1992); R. T. Batey, M. Inada, E. Kujawinski, J. D. Puglisi, J. R. Williamson, *ibid.*, p. 4515; M. J. Michnicka, J. W. Harper, G. C. King, *Biochemistry* **32**, 395 (1993); S. Quant *et al.*, *Tetrahedron Lett.* **36**, 6649 (1994).
6. R. Brüschweiler, C. Griesinger, R. R. Ernst, *J. Am. Chem. Soc.* **111**, 8034 (1989).
7. M. Linder, A. Höhener, R. R. Ernst, *J. Chem. Phys.* **73**, 4959 (1980).
8. K. Schmidt-Rohr, *J. Am. Chem. Soc.* **118**, 7601 (1996); \_\_\_\_\_, *Macromolecules* **29**, 3975 (1996).
9. X. Feng, Y. K. Lee, D. Sandstrom, M. Eden, A. Sebald, M. H. Levitt, *Chem. Phys. Lett.* **257**, 314 (1996); G. Dabbagh, D. P. Weliky, R. Tycko, *ibid.* **27**, 6183 (1994).
10. N. Bloembergen, E. M. Purcell, R. V. Pound, *Phys. Rev.* **73**, 679 (1948).
11. L. G. Werbelow and D. M. Grant, *Adv. Magn. Reson.* **9**, 189 (1974).
12. A. Abragam, *The Principles of Nuclear Magnetism* (Clarendon Press, Oxford, 1961).
13. J. Cavanagh, W. J. Fairbrother, A. G. Palmer III, N. J. Skelton, *Protein NMR Spectroscopy* (Academic Press, San Diego, 1996).
14. L. E. Kay, D. A. Torchia, A. Bax, *Biochemistry* **28**, 8972 (1989); G. M. Clore, P. C. Driscoll, P. T. Wingfield, A. Gronenborn, *ibid.* **29**, 7378 (1990).
15. G. Lipari and A. J. Szabo, *J. Am. Chem. Soc.* **104**, 4546 (1982); N. Tjandra, A. Szabo, A. Bax, *ibid.* **118**, 6986 (1996); D. E. Woessner, *J. Chem. Phys.* **36**, 1 (1962); *ibid.* **37**, 647 (1962); G. Barbato, M. Ikura, L. E. Kay, R. W. Pasto, A. Bax, *Biochemistry* **31**, 5269 (1992); I. Q. H. Phan, J. Boyd, I. D. Campbell, *J. Biomol. NMR* **8**, 369 (1996).
16. A. C. Wang and A. Bax, *J. Am. Chem. Soc.* **117**, 1810 (1995).
17. A. Bax and M. Ikura, *J. Biomol. NMR* **1**, 99 (1991).
18. A. v. d. Locht *et al.*, *EMBO J.* **14**, 5149 (1995).
19. M. Maurer, V. Bellingier, T. Naumann, A. Diener, C. Griesinger, in preparation.
20. Z. Madi and R. R. Ernst, WTEST program package, Eidgenössische Technische Hochschule Zürich, Switzerland, 1989.
21. J. R. Tolman, J. M. Flanagan, M. A. Kennedy, J. H. Prestegard, *Proc. Natl. Acad. Sci. U.S.A.* **92**, 9279 (1995); N. Tjandra, S. Grzesiek, A. Bax, *J. Am. Chem. Soc.* **118**, 6264 (1996).
22. N. Tjandra, H. Kuboniwa, H. Ren, A. Bax, *Eur. J. Biochem.* **230**, 1014 (1995).
23. T. M. Duncan, *A Compilation of Chemical Shift Anisotropies* (Farragut Press, Chicago, 1990).
24. M. D. Lumsden *et al.*, *J. Am. Chem. Soc.* **116**, 1403 (1994); C. J. Hartzell, M. Whitfield, T. G. Oas, G. P. Drobny, *ibid.* **109**, 5966 (1987).
25. N. Janes, S. Ganapathy, E. Oldfield, *J. Magn. Reson.* **54**, 111 (1983).
26. L. J. Smith *et al.*, *J. Mol. Biol.* **255**, 494 (1996).
27. L. Emsley and G. Bodenhausen, *J. Magn. Reson.* **82**, 211 (1989); *Chem. Phys. Lett.* **165**, 469 (1989).
28. R. Fu and G. Bodenhausen, *Chem. Phys. Lett.* **245**, 415 (1995).
29. Supported by the Fonds der Chemischen Industrie and in part by the DFG under grant 1211/6-1. M.H. acknowledges a Ph.D. fellowship by the Fonds der Chemischen Industrie. We thank M. Maurer for providing the assignments and the NMR structural data of rhodniin in solution. We are grateful for continuous support by T. Keller and W. Bernel, Bruker, Karlsruhe, Germany.

10 December 1996; accepted 14 March 1997

## Large Molecular Third-Order Optical Nonlinearities in Polarized Carotenoids

Seth R. Marder,\* William E. Torruellas,†  
Mirelle Blanchard-Desce, Vincent Ricci, George I. Stegeman,  
Sharon Gilmour, Jean-Luc Brédas, Jun Li, Greg U. Bublitz,  
Steve G. Boxer

Garito and co-workers have suggested a mechanism to dramatically increase the second hyperpolarizability,  $\gamma$ , in linear  $\pi$ -electron-conjugated molecules. Polarization is introduced that leads to a difference between the dipole moments of the molecule's ground state and excited state. Here a series of carotenoids was examined that had increasing intramolecular charge transfer (ICT) from the polyenic chain to the acceptor moiety in the ground state, and  $\gamma$  was measured for these compounds as a function of wavelength by third-harmonic generation. The compound with the greatest ICT exhibited a 35-fold enhancement of  $\gamma_{\text{max}}$  (the  $\gamma$  measured at the peak of the three-photon resonance) relative to the symmetric molecule  $\beta$ -carotene, which itself has one of the largest third-order nonlinearities known. Stark spectroscopic measurements revealed the existence of a large difference dipole moment,  $\Delta\mu$ , between the ground and excited state. Quantum-chemical calculations underline the importance of interactions involving states with large  $\Delta\mu$ .

Molecules with large third-order optical nonlinearities (characterized by large second hyperpolarizabilities,  $\gamma$ ) are required for photonic applications including all-optical switching, data processing, and eye and sensor protection. In contrast to second-order nonlinear materials, for which the basic structure-property relations are both relatively well understood and well explored, for third-order materials a comparable level of understanding is only just emerging. Garito and co-workers have suggested a mechanism to dramatically in-

crease  $\gamma$  (1, 2), and they calculated that polarized polyenes could have very large  $\gamma$ , relative to unsubstituted polyenes of comparable length, because of symmetry breaking. A parallel situation exists in semiconductor quantum wells where asymmetrization has led to some of the largest second- and third-order nonlinearities ever observed in the mid- to far-infrared portion of the spectrum, both with and without the presence of permanent dc fields (3–5). The results of recent computational and experimental studies on small model systems agree with the predictions of Garito *et al.* (6–9). Nonetheless, molecules that exhibit extremely large  $\gamma$  according to the mechanism predicted by Garito *et al.* are still quite unusual (10–12). Indeed,  $\gamma$  values are still, perhaps with rare exceptions (13), not sufficiently large for realistic applications to ultrafast information-processing optical devices. Here we explored the hypothesis of Garito *et al.* further and found that large enhancements in  $\gamma$  can be achieved in a variety of acceptor-substituted carotenoids as determined by wavelength-dependent third-harmonic generation experiments (THG).

Several groups have shown from a sum-over-states analysis of  $\gamma$  derived from perturbation theory that three classes of terms

S. R. Marder, Beckman Institute, California Institute of Technology, Pasadena, CA 91125, USA, and Jet Propulsion Laboratory, California Institute of Technology, Pasadena, CA 91109, USA.

W. E. Torruellas, V. Ricci, G. I. Stegeman, Center for Research on Education, Optics, and Lasers, University of Central Florida, 4000 Central Florida Boulevard, Orlando, FL 32816, USA.

M. Blanchard-Desce, Ecole Normale Supérieure, Département de Chimie (Unité de Recherche Associée 1679 CNRS), 24 rue Lhomond 75231, Paris Cedex 05, France.

S. Gilmour, Jet Propulsion Laboratory, California Institute of Technology, Pasadena, CA 91109, USA.

J.-L. Brédas and J. Li, Center for Research on Molecular Electronics and Photonics, Université de Mons-Hainaut, Place du Parc 20, B-7000 Mons, Belgium.

G. U. Bublitz and S. G. Boxer, Department of Chemistry, Stanford University, Stanford, CA, 94305, USA.

\*To whom correspondence should be addressed.  
†Present address: Department of Physics, Washington State University, Pullman, WA 99164, USA.

should dominate the third-order nonlinear optical response of linear conjugated molecules. In particular, it was shown that in the static limit

$$\gamma \propto -\left(\frac{\mu_{ge}^4}{E_{ge}^3}\right) + \sum_{e'} \left(\frac{\mu_{ge}^2 \mu_{ce'}^2}{E_{ge}^2 E_{ce'}}\right) + \left[\frac{\mu_{ge}^2 (\mu_{ce} - \mu_{gg})^2}{E_{ge}^3}\right] \quad (1)$$

N                      TP                      D

where *g* labels the ground state, *e* and *e'* label the two excited states, and  $\mu$  and *E* are the dipole matrix element and transition energy, respectively, between the labeled states. Hence, the three-state expression for  $\gamma$  consists of three terms, one negative (N), a two-photon term (TP), and a dipolar term (D). The D term is zero for centrosymmetric polyenes where  $\mu_{ee} = \mu_{gg} = 0$ , and in this case, TP > |N| and thus  $\gamma$  is positive (6–9).

For neutral cyanine-like molecules (in which one-half of a charge is transferred from the donor to the acceptor in the ground state)  $\mu_{ee} = \mu_{gg} \neq 0$ , and thus the D term is also negligible, and, as |N| > TP,  $\gamma$  is negative (6–9). If for polarized polyenes the D term were large, then it could have a large positive contribution to  $\gamma$ . Relatively close to the sym-

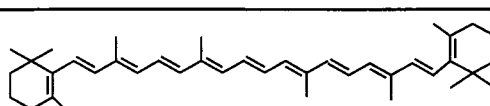
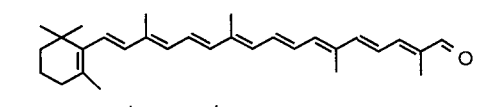
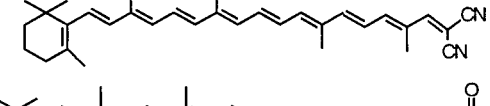
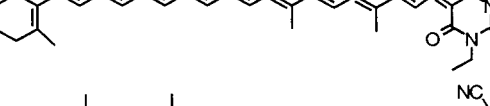
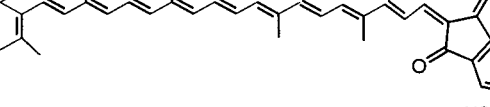
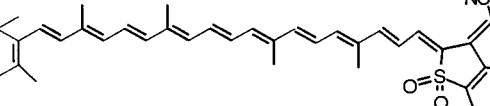
metrical polyene limit, it is predicted that polarization of the molecule leads to the D + TP terms increasing more rapidly than |N|, and, as Garito *et al.* predicted (1, 2), large enhancements in  $\gamma$  should be possible (1, 2, 6–9).

We used  $\beta$ -carotene, **1**, as our starting reference symmetrical, “unsubstituted” polyene to design and synthesize molecules in which one end was substituted with increasingly stronger acceptors, thereby increasing the extent of intramolecular charge transfer (ICT) from the polyenic chain to the acceptor moiety in the ground state (14, 15) (Table 1, top to bottom).  $\beta$ -Apo-carotenal, **2**, was commercially available at the time of this study, and compound **3** has been reported (16). Attempts to react **2** with the active methylene precursors for the acceptors for compounds **4** to **6** under a variety of Knoevenagel conditions failed to give appreciable yields of the desired product, presumably because of steric interactions between groups on the acceptor and the methyl group on the carbon  $\alpha$  to the aldehyde carbon. Accordingly, we first produced a homolog of **2** containing one additional double bond, and then the Knoevenagel condensations proceeded smoothly. After purification by chromatogra-

phy and recrystallization, the compounds were analyzed by <sup>1</sup>H nuclear magnetic resonance, mass spectroscopy, optical [ultraviolet-visible and near-infrared (NIR)] spectroscopy, and elemental analysis, all of which gave data consistent with the proposed structures.

The second hyperpolarizability as a function of wavelength for each of the six molecules in Table 1 was determined by THG. Our experimental apparatus and procedures have been described in (17). A plot of the spectrum of  $\gamma$  for **1** and **6** is shown in Fig. 1. Table 1 summarizes the position of the absorption maxima ( $\lambda_{max}$ ) and  $\gamma_{max}$  values for compounds **1** through **6**, whose position typically occurs at the three-photon resonance ( $3 \times h\nu$ ). There is a dramatic increase in  $\gamma_{max}$  values of the compounds with increasing acceptor strength relative to  $\beta$ -carotene. For example, compound **6** has a  $\gamma_{max}$  35 times that of  $\beta$ -carotene. The incorporation of the acceptor introduces charge-transfer character into the  $\pi$ - $\pi^*$  transition, leading to a bathochromic shift. As a result, for compound **6** this transition is shifted 276 nm to a longer wavelength than the  $\pi$ - $\pi^*$  transition observed for  $\beta$ -carotene, limiting the transmission window before the onset of absorption because of vibrational overtones.

**Table 1.** Numbering scheme, structures, and  $\gamma_{max}$  at the peak of the three-photon resonance of compounds, relative to  $\beta$ -carotene, as measured by THG. The values of  $\gamma_{max}$  are calculated from the experimental values of the relative magnitude of the third-order susceptibility of a thin-film polymer sample containing the compound as a solute. The susceptibilities are referenced to fused-silica for which a susceptibility of  $1.5 \times 10^{-14}$  esu was assumed. The concentration of chromophores in the samples was  $3.6 \times 10^{20}$  molecule  $cm^{-3}$ . The  $\gamma_{max}$  values for the compounds have not been corrected for the local field factor (that is, a local field factor of unity was assumed).

Compound	Chemical structure	$\lambda_{max}$ (nm)	$\gamma_{max}$ ( $\times 10^{-32}$ esu)
1		464	1
2		464	1.9
3		540	2.5
4		590	8.1
5		680	19
6		740	35

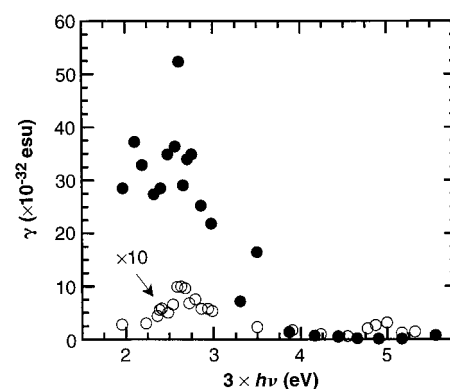


**Fig. 1.** An example of a THG spectrum for compounds **1** (open circles) and **6** (filled circles). The data for **1** were multiplied by a factor of 10 to increase their visibility on the plot. The estimated precision of the data is  $\pm 10\%$ . We obtained the THG spectra using an injection-seeded Nd:yttrium-aluminum-garnet Q-switched laser, frequency-doubled, pumping a nanosecond dye laser, the output of which was focused into a H<sub>2</sub> Raman cell to produce infrared wavelengths between 900 and 1500 nm. The dye laser beam was also combined with the nonconverted fundamental at 1064 nm to produce wavelengths in the range of 1500 to 2100 nm in a LiO<sub>3</sub> down-converter. The NIR radiation was then focused into a vacuum cell where the thin film samples, deposited on top of fused silica substrates, were rotated. The generated third harmonic was collected into and dispersed by a 0.25-m spectrometer and detected with a photomultiplier. Esu, electrostatic unit;  $3 \times h\nu$ , three-photon resonance.

We hypothesize that the large increase in  $\gamma$  for the compounds in this study relative to  $\beta$ -carotene arises from the introduction of a large D term. Electroabsorption (Stark) spectroscopy provides a method for determining the change in dipole moment ( $\Delta\mu = \mu_{ee} - \mu_{gg}$ ) upon a molecular transition from the ground to an excited state. For an isotropic, immobilized sample  $\Delta\mu$  gives rise to a  $\Delta A$  (Stark) spectrum whose line shape resembles the second derivative of the absorption spectrum (18). The Stark spectrum for compound **6** taken in 2-methyltetrahydrofuran solution at 77 K (shown in Fig. 2B) has a dominant second derivative line shape (compare with Fig. 2C). The analysis of the spectrum reveals a large  $|\Delta\mu|$  that changes across the absorption band, decreasing from the red to the blue edge of the spectrum.

From a simultaneous fit of the absorption and Stark spectra, we can estimate  $|\Delta\mu| = 40 \pm 5$  D for the region of maximum absorption (that is, around 13,000 to 14,000  $\text{cm}^{-1}$ ). Both the value of  $|\Delta\mu|$  and the inhomogeneity across the absorption band are confirmed by a comparison of the Stark spectrum in Fig. 2B with the higher order Stark spectrum (19). Interestingly, compound **4** gave values of  $|\Delta\mu|$  similar to those of **6**, and

yet  $\gamma_{\text{max}}$  for **4** is a factor of 4.3 smaller. Assuming the D term is the dominant contribution to  $\gamma$ , this difference can be explained by the offsetting effect of the  $\mu_{ge}^2/E_{ge}^3$  factor in the D term. For compound **6**,  $\mu_{ge} = 14$  D and  $\lambda_{\text{max}} = 740$  nm, whereas for compound **4**,  $\mu_{ge} = 10$  D and  $\lambda_{\text{max}} = 590$  nm. Thus, the ratio of  $\mu_{ge}^2/E_{ge}^3$  for compound **6** relative to compound **4** is 3.9, in agreement with our THG results. Both  $\mu_{ge}$  and  $\lambda_{\text{max}}$  are affected by the relative extent of polarization in the ground-states structures, but for compound **6** it is also possible that the introduction of the benzo ring fused to the five-membered ring containing the sulfone and the dicyanomethylene can lead to increased delocalization that will also influence each of the components of the D term.

In order to explore the electronic structure and optical properties of polarized carotenoids, we performed correlated quantum-chemical calculations on a 10-double bond polyene capped at one end by a dicyanovinylene acceptor group (Fig. 3). The calculations were carried out at the INDO-SDCI (intermediate neglect of differential overlap–single and double configuration interaction) level with geometry optimization (9). In some of our recent computational studies, we showed that an external electric field aligned along the molecular dipole moment,  $F_{\text{ext}}$  in Fig. 3, is very successful in simulating the influence of acceptor strength (9). We obtained reasonably good agreement between the calculated and observed  $S_0 \rightarrow S_1$  transition energy for compound **6** when this external field is  $F_{\text{ext}} = 2 \times 10^7$  V  $\text{cm}^{-1}$  (1.9 eV calculated versus 1.7 eV experimental). Therefore, we fixed  $F_{\text{ext}}$  at this value and calculated a variety of other observables

(using a damping factor,  $\Gamma$ , of 0.1 eV) and obtained theoretical predictions that agree well with experimental data. For example: (i)  $S_0 \rightarrow S_2$  transition energy (2.9 eV calculated versus 2.9 eV experimental); (ii)  $\mu_{ge}(S_0 \rightarrow S_1)$  (16.5 D calculated versus 14 D measured); and (iii) dipole moment difference between  $S_1$  and  $S_0$  (41 D calculated versus  $40 \pm 5$  D measured).

We have further evaluated the static and dynamic molecular polarizabilities using the sum-over-states approach and  $F_{\text{ext}} = 2 \times 10^7$  V  $\text{cm}^{-1}$  in the manner described in (9). The peak THG  $\gamma$  value, occurring at a fundamental energy of 0.6 eV, was  $\sim 36 \times 10^{-32}$  electrostatic unit (esu); this value can be compared with a value of  $0.76 \times 10^{-32}$  esu calculated for  $\beta$ -carotene (20). The calculated enhancement factor is thus 47, which again compares well with the experimental value of 35. The overall agreement between calculated and experimental values lends confidence in the reliability of our theoretical approach.

We have fitted the fully converged sum-over-states  $\gamma$  values described above to a simplified three-term expression similar to the relation in Eq. 1. Although the three-term expression gives a satisfactory sense of the dependence of  $\gamma$  on ground-state ICT, it does not provide satisfactory agreement with the magnitude of the fully converged  $\gamma$  values and overestimates  $\gamma$  by  $\sim 50\%$ . However, an excellent fit is obtained if we consider an additional dipolar term  $D'$  of the following form:

$$D' = \frac{\mu_{ge}(\mu_{ee} - \mu_{gg})\mu_{e'e'}\mu_{e'g}}{E_{ge}^2 E_{e'e}} + \frac{\mu_{ge}\mu_{e'e}(\mu_{e'e'} - \mu_{gg})\mu_{e'g}}{E_{ge} E_{e'e}^2} \quad (2)$$

which leads to an overall negative contribution to  $\gamma$ . In these  $D'$  terms, the ground state is coupled strongly not only to the lowest excited state (e, which is  $S_1$ ) but also to the next excited state ( $e'$ , which is  $S_2$ ), and  $S_1$  and  $S_2$  are also strongly coupled to one another as shown schematically in Fig. 4 [that a second excited state becomes important with increasing chain length has already been shown in the case of diphenylacetylene compounds (21)]. The major result of the fit, however, is that the large  $\gamma$  enhancement in the acceptor-substituted  $\beta$ -carotenoids is due to the dipolar terms, a concept originally introduced by Garito *et al.* (1, 2).

In this class of carotenoid molecules, the polarization created by the internal field associated with the presence of strong electron acceptors results in significant bathochromic shifts and large enhancements of  $\gamma$  relative to  $\beta$ -carotene. For compound **6**, we

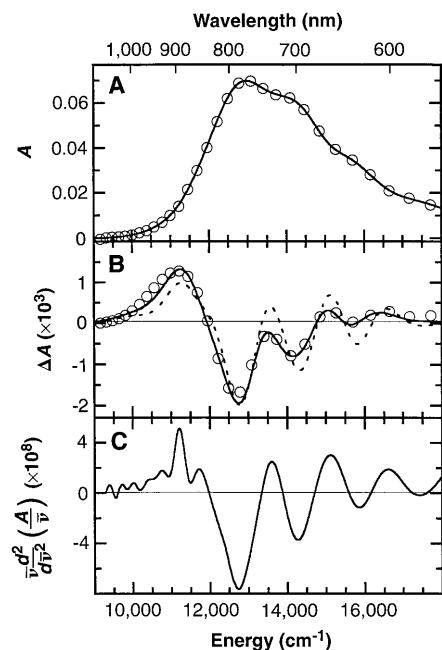


**Fig. 2.** (A) Absorption spectrum; (B) Stark spectrum (applied external field of 0.683 MV  $\text{cm}^{-1}$ ); (C) frequency-weighted ( $\bar{\nu}$ -weighted) second derivative of the absorption spectrum of compound **6** taken at 77 K in a frozen glass of 2-methyltetrahydrofuran. In (A) and (B) the data are represented by open circles, and the result of the simultaneous best fit of the  $A$  and  $\Delta A$  data [from which  $|\Delta\mu|$  and  $\Delta\alpha$  are obtained (18)] are superimposed as solid lines. The broken line in (B) represents the results of fitting the entire spectrum with only one single value of  $|\Delta\mu|$  and  $\Delta\alpha$ .

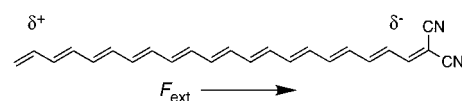


**Fig. 3.** Model compound polarized by an external electric field used in INDO-SDCI calculations.

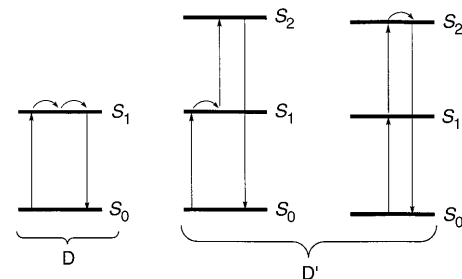


**Fig. 4.** Schematic of key virtual transitions contributing to the third-order optical nonlinearity of highly polarized carotenoids.

observed an enhancement in  $\gamma$  by a factor of 35 relative to  $\beta$ -carotene, which itself has one of the largest molecular  $\gamma$  values reported (10–12, 22). We have realized this enhancement of  $\gamma$  without large increases in either the molecular length or the molecular volume, albeit with some loss of transparency. Although it is unlikely that these specific compounds will be used to make practical devices because of their inherent instability with respect to long-term exposure to air and light, our results do validate and expand on the predictions of Garito *et al.* and thus suggest a clear strategy to further enhance  $\gamma$  in a variety of  $\pi$ -conjugated systems.

## REFERENCES AND NOTES

1. A. F. Garito, J. R. Heflin, K. Y. Yong, O. Zamani-Khamiri, *Proc. Soc. Photo. Opt. Instrum. Eng.* **971**, 2 (1988).
2. \_\_\_\_\_, in *Organic Materials for Nonlinear Optics*, R. A. Hann and D. Bloor, Eds. (Royal Society of Chemistry, London, 1989), p. 16.
3. M. M. Fejer, S. J. B. Yoo, R. L. Byer, A. Harwit, J. S. Harris, *Phys. Rev. Lett.* **62**, 1041 (1989).
4. G. Almogly and A. Yariv, *Opt. Lett.* **19**, 1828 (1994).
5. F. Capasso, C. Sirtori, A. Y. Cho, *IEEE J. Quantum Electron.* **30**, 1313 (1994).
6. B. M. Pierce, *Proc. Soc. Photo. Opt. Instrum. Eng.* **1560**, 148 (1991).
7. C. W. Dirk, L.-T. Cheng, M. G. Kuzyk, *Int. J. Quantum Chem.* **43**, 27 (1992).
8. S. R. Marder, *et al.*, *Science* **265**, 632 (1994).
9. F. Meyers, S. R. Marder, B. M. Pierce, J.-L. Brédas, *J. Am. Chem. Soc.* **116**, 10703 (1994).
10. J. Messier *et al.*, *Nonlinear Opt.* **2**, 53 (1992).
11. G. Puccetti, M. Blanchard-Desce, I. Ledoux, J.-M. Lehn, J. Zyss, *J. Phys. Chem.* **97**, 9385 (1993).
12. M. Blanchard-Desce *et al.*, *Nonlinear Opt.* **10**, 23 (1995).
13. C. Halvorson *et al.*, *Science* **265**, 1215 (1994).
14. M. Blanchard-Desce *et al.*, *J. Photochem. Photobiol. A*, in press.
15. M. Blanchard-Desce *et al.*, *Chem. Eur. J.*, in press.
16. S. Gilmour, S. R. Marder, B. G. Tiemann, L.-T. Cheng, *J. Chem. Soc. Chem. Commun.* **1993**, 432 (1993).
17. S. Aramaki, W. E. Torruellas, R. Zanoni, G. I. Stegeman, *Opt. Commun.* **85**, 527 (1991).
18. The change in absorption,  $\Delta A$ , upon application of an electric field can be decomposed into contributions proportional to the first and second derivative of the molecule's absorption spectrum, which are related to  $\Delta\alpha$  (the change in polarizability between the ground and excited state) and  $|\Delta\mu|$ , respectively. See W. Liptay, in *Excited States*, E. C. Lim, Ed. (Academic Press, New York, 1974), pp. 129–229.
19. K. Lao, L. J. Moore, H. Zhou, S. G. Boxer, *J. Phys. Chem.* **99**, 496 (1995).
20. D. Beljonne *et al.*, *Phys. Rev. B*, in press.
21. C. Dehu, F. Meyers, J. L. Brédas, *J. Am. Chem. Soc.* **115**, 6198 (1993).
22. J. P. Hermann and J. Ducuing, *J. Appl. Phys.* **45**, 5100 (1974).
23. This work was supported by the Air Force Office of Scientific Research, the National Science Foundation Chemistry Division (S.G.B.), the Division of Materials Research (S.R.M.), and the Beckman Institute. The research described in this report was performed in part at the Jet Propulsion Laboratory, California Institute of Technology, as part of its Center for Space Microelectronics Technology and was supported by the Ballistic Missiles Defense Initiative Organization, Innovative Science and Technology Office, through a contract with NASA. The work at Mons, Belgium, is carried out within the framework of the Belgium Prime Minister Office

of Science Policy "Pôle d'Attraction Interuniversitaire en Chimie Supramoléculaire et Catalyse" and was supported in part by the Belgium National Fund for Scientific Research and by IBM–Belgium Academic Joint Study. We thank F. Hoffman–

LaRoche Ltd. for a generous sample of  $\beta$ -apocarotenal and G. Zerbi and M. Barzoukas for helpful discussions.

22 January 1997; accepted 7 April 1997

## Europa's Differentiated Internal Structure: Inferences from Two Galileo Encounters

J. D. Anderson,\* E. L. Lau, W. L. Sjogren, G. Schubert, W. B. Moore

Doppler data generated with the Galileo spacecraft's radio carrier wave during two Europa encounters on 19 December 1996 (E4) and 20 February 1997 (E6) were used to measure Europa's external gravitational field. The measurements indicate that Europa has a predominantly water ice–liquid outer shell about 100 to 200 kilometers thick and a deep interior with a density in excess of about 4000 kilograms per cubic meter. The deep interior could be a mixture of metal and rock or it could consist of a metal core with a radius about 40 percent of Europa's radius surrounded by a rock mantle with a density of 3000 to 3500 kilograms per cubic meter. The metallic core is favored if Europa has a magnetic field.

Before the Galileo mission to Jupiter there was little information on Europa's interior structure. Its mean density of  $3018 \pm 35 \text{ kg m}^{-3}$ , determined from previous Jupiter missions (1), is consistent with an interior of hydrated silicate minerals with a thin ice cover, or alternatively an interior of dehydrated silicate minerals with a thick ice cover (2). Here we report gravitational data from two close passes of Europa by the Galileo spacecraft, E4 and E6, that show that Europa has a more complicated internal structure. Recent Galileo data have shown that Ganymede is differentiated, most likely into a three-layer structure with a large metallic core, a silicate mantle and a thick outer layer of ice (3); Io has a large metallic core (4); and Callisto is essentially a uniform mixture of ice and rock (5).

The Galileo spacecraft flew by Europa on 19 December 1996 (E4) and 20 February 1997 (E6) and measured the Doppler shift in the spacecraft's radio carrier wave. We analyzed these data by fitting a parameterized orbital model, including Europa's gravitational field, to the radio Doppler data by weighted nonlinear least squares (6). Europa's external gravitational field was modeled by the standard spherical harmonic representation of the gravitational potential (7). For the assumption that the origin of coordinates is at the center of mass and that the orientation of

Europa's principal axes is known because it rotates synchronously, only three gravity parameters are needed to specify the gravitational potential through the second degree and order (8).

For the two encounters (9) the two gravity coefficients are highly correlated, so we imposed the a priori hydrostatic constraint that  $J_2$  is  $10/3$  of  $C_{22}$ . Also, because of an inconsistency in results for E4 and E6, analyzed independently, we added two third-degree gravity coefficients  $J_3$  and  $C_{33}$  to the fitting model. The addition of these two harmonics makes the results (Table 1) more consistent and possibly indicates that there are significant nonhydrostatic components in Europa's gravitational field perturbing  $J_2$  and  $C_{22}$ . The Jupiter-Europa distance was 671,567,992 m during E4 and 671,569,331 m during E6, so the Jupiter tidal force at Europa's surface differed by a fractional amount,  $6 \times 10^{-6}$ , between the two encounters. This difference is too small to account for the inconsistency in the results. Given that neither E4 nor E6 are ideal encounters for a gravity field determination, it is not possible to relax the  $J_2 = (10/3)C_{22}$  a priori hydrostatic constraint or to explore the physical significance of the inconsistency between E4 and E6 in more detail. Additional close encounters with Europa, perhaps with a Galileo extended mission or a future orbiter mission, could reveal the true nature of this inconsistency.

Because of the a priori constraint, the values of  $J_2$  and its uncertainty are nearly  $10/3$  of  $C_{22}$  (Table 1). There is essentially 1 degree of freedom per encounter in the second-degree field. The measured gravity signals corresponding to the values of  $J_2$ ,  $C_{22}$ ,

J. D. Anderson, E. L. Lau, W. L. Sjogren, Jet Propulsion Laboratory, California Institute of Technology, Pasadena, CA 91109–8099, USA.  
G. Schubert and W. B. Moore, Department of Earth and Space Sciences, Institute of Geophysics and Planetary Physics, University of California, Los Angeles, CA 90095–1567, USA.

\*To whom correspondence should be addressed.